FACULDADE DE MEDICINA DA UNIVERSIDADE DE COIMBRA

TRABALHO FINAL DO 6º ANO MÉDICO COM VISTA À ATRIBUIÇÃO DO GRAU DE MESTRE NO ÂMBITO DO CICLO DE ESTUDOS DE MESTRADO INTEGRADO EM MEDICINA

ANA RITA DE BRITO MACHADO

VISUAL CORTICAL ATROPHY IN RETINITIS PIGMENTOSA PATIENTS WITH PARTIALLY PRESERVED VISION: A VOXEL-BASED MORPHOMETRY STUDY

ARTIGO CIENTÍFICO

ÁREA CIENTÍFICA DE NEUROCIÊNCIAS

TRABALHO REALIZADO SOB A ORIENTAÇÃO DE:
MIGUEL DE SÁ E SOUSA DE CASTELO BRANCO
FÁBIO DANIEL SANTOS FERREIRA

FEVEREIRO 2016

VISUAL CORTICAL ATROPHY IN RETINITIS PIGMENTOSA PATIENTS WITH PARTIALLY PRESERVED VISION: A VOXEL-BASED MORPHOMETRY STUDY

Ana Rita Machado[1], Fábio Ferreira[2], Andreia Pereira[2], Sónia Ferreira[2], Bruno Quendera[3], Eduardo Silva[1] , Miguel Castelo-Branco[1,2,3]

[1] Faculty of Medicine, University of Coimbra, Portugal

[2] Visual Neuroscience Laboratory, Centre for Ophthalmology, Institute for Biomedical Imaging and Life Sciences (IBILI), Faculty of Medicine, University of Coimbra, Portugal

[3]Institute of Nuclear Sciences Applied to Health (ICNAS), Brain Imaging Network of Portugal, University of Coimbra, Portugal

Ana Rita de Brito Machado
Correio electrónico: ritabritomachado@gmail.com

Table of Contents

Abstract

Retinitis Pigmentosa is a group of hereditary retinal dystrophy disorders associated with progressive visual field loss. In the typical form, retinal degeneration starting at photoreceptors rods in the mid-periphery of the retina causes peripheral visual field defects. Twenty-seven patients and forty healthy controls were examined to determine whether progressive peripheral vision loss in Retinitis Pigmentosa patients with partially preserved vision leads to structural cortical changes. Retinal thickness and retinal nerve fiber layer (RNFL) thickness were assessed with optical coherence tomography (OCT). T1 high-resolution brain anatomical magnetic resonance images from each subject were obtained on a 3-T scanner and processed using SPM8. A whole brain voxel-wise statistical comparison of grey matter volume between the two groups was performed using two different contrasts (controls > patients and patients > controls). Significant statistical difference was found for retinal thickness ($P < 0.05$), but not for RNFL thickness ($p > 0.05$) between groups. Grey matter atrophy was observed in the left pericalcarine cortex, cuneus gyrus, posterior cingulate gyrus, right pericalcarine cortex and lingual gyrus ($p < 0.001$, uncorrected for multiple comparisons, at the whole brain level) of Retinitis Pigmentosa patients. Further analysis with a family-wise error (FWE) correction for multiple comparisons revealed grey matter atrophy in the left pericalcarine cortex, cuneus gyrus and lingual gyrus ($p < 0.05$). Grey matter hypertrophy was not observed. While the retinal thinning observed is consistent with photoreceptor degeneration, no evidence of structural alteration of RNFL was found. The locations of the grey matter atrophy in visual primary and association cortices are coincident with the profile of peripheral visual field deficit seen in Retinitis Pigmentosa. The cortical atrophy registered is likely to be a result of disuse-driven neuronal atrophy and/or transneuronal degeneration of the visual pathway. These findings may have clinical implications for disease management.

Keywords: Retinitis Pigmentosa; visual field; visual cortex; optical coherence tomography; voxel-based morphometry; grey matter volume.

Resumo

A Retinopatia Pigmentar é um grupo de distúrbios hereditários de distrofia da retina associado a perda progressiva de campo visual. Na forma típica, a degeneração da retina que se inicia pelos fotoreceptores bastonetes na médio-periferia da retina causa defeitos periféricos de campo visual. Vinte e sete doentes e quarenta controlos saudáveis foram examinados para determinar se a perda progressiva de visão periférica nos doentes com Retinopatia Pigmentar com visão parcialmente preservada conduz a alterações estruturais corticais. As espessuras da retina e da camada de fibras nervosas da retina (CFNR) foram avaliadas com tomografia de coerência óptica (TCO). As imagens cerebrais anatómicas de ressonância magnética de cada participante foram obtidas num scanner 3-T utilizando a sequência T1 de alta resolução e processadas usando o SPM8. Foi realizada uma comparação estatística voxel-a-voxel do volume de matéria cinzenta entre os dois grupos, examinando todo o cérebro, usando dois contrastes simétricos (controlos > doentes e doentes > controlos). Foi encontrada uma diferença estatística significativa para a espessura da retina entre os grupos ($p < 0.05$) , mas não para a espessura da CFNR ($p > 0.05$). Na análise exploratória inicial, foi observada atrofia de matéria cinzenta no córtex pericalcarino esquerdo, giro cúneos, giro cingulado posterior, córtex pericalcarino direito e giro lingual ($p < 0.001$, com correção apenas para clusters de 100 vóxeis) dos doentes com Retinopatia Pigmentar. Uma análise confirmatória subsequente com correção para comparações múltiplas "family-wise error" (FWE) demonstrou atrofia de matéria cinzenta no córtex pericalcarino esquerdo, giro cúneos e giro lingual ($p < 0.05$). Não foi observada hipertrofia de matéria cinzenta. Enquanto que a redução da espessura da retina observada é consistente com a degeneração de fotoreceptores, não foi

encontrada evidência de alteração estrutural da CFNR. A localização das áreas de atrofia de matéria cinzenta nos córtex visuais primário e de associação coincidem com o perfil de défice periférico de campo visual observado na Retinopatia Pigmentar. A atrofia cortical observada é provavelmente um resultado de atrofia neuronal induzida pelo desuso e/ou degeneração transneuronal da via visual. Estes achados podem ter implicações clínicas no controlo da patologia.

Palavras-chave: Retinopatia Pigmentar; campo visual; córtex visual; tomografia de coerência óptica; voxel-based morphometry; volume de matéria cinzenta.

List of abbreviations

AMD Age-related Macular Degeneration

CSF Cerebrospinal Fluid

CTL Controls

FWE Family Wise Error

GM Grey Matter

MRI Magnetic Resonance Imaging

OCT Optical Coherence Tomography

POAG Primary Open Angle Glaucoma

RGC Retinal Ganglion Cells

RNFL Retinal Nerve Fiber Layer

RP Retinitis Pigmentosa

TIV Total Intra-cranial Volume

VBM Voxel-Based Morphometry

VFD Visual Field Defect(s)

WM White Matter

Introduction

Retinitis Pigmentosa (RP) is a cause of human visual disability due to peripheral visual field defects (VFD). The non-syndromic form of RP has a worldwide prevalence of about 1/4000 individuals (1-4). It is a a group of inherited retinal dystrophy disorders characterised by photoreceptor degeneration with subsequent vision loss (3). In the typical form of RP, retinal degeneration starts at photoreceptor rods in the mid-periphery and advances towards the macula and fovea, further affecting the photoreceptor cones. This form is also described as a rod-cone dystrophy and its clinical hallmark is progressive peripheral visual field loss. Patients initially present nyctalopia, followed by the progressive peripheral VFD, and eventually blindness. The age of onset is highly variable, ranging from childhood to mid-adulthood (1, 2).

Voxel-based morphometry (VBM) is an automated technique (5-7) that has been used to study grey matter (GM) volume differences between controls and patients with VFD acquired later in life. However, some of those studies have focused on patients whose late VFD has already evolved to blindness. Moreover, the neuro-ophthalmological pathologies causing blindness were multiple, leading to different mechanisms of brain adaptation to the visual loss. (8-10). VBM studies of structural cortical alterations on patients with partially preserved vision due to VFD has mainly concerned glaucoma, characterised by peripheral VFD, and age-related macular degeneration (AMD), characterised by central or pericentral VFD. In the first study addressing this issue, GM atrophy in the approximate retinal lesion projection zones in the visual cortex was reported in AMD and glaucoma patients (11). Several other studies have found cortical degeneration in patients with central retina degeneration (12-14). Furthermore, a morphometry study involving hereditary macular dystrophies patients with central scotomata found a correlation between scotomata size and GM loss, suggesting that the lack of visual input may induce the GM atrophy (13). Regarding peripheral VFD, the

focus of morphometry studies has been mainly on glaucoma (11, 15-18). Li et al. further analysed the extraoccipital cortex in progressive stages of primary open angle glaucoma (POAG) and reported no GM volume changes in the early stage, but GM reduction was found in multiple cortical brain regions, including the primary visual cortex, in the advanced-late stage POAG group. Conversely, there was a GM hypertrophy near the most damaged brain region, which may reflect the possibility of structural reorganisation (15). Similar studies also reported volumetric losses and gains in several brain regions in glaucoma (15, 16, 18). To the best of our knowledge, only one study has investigated the presence of visual cortex atrophy due to peripheral VFD in disorders other than glaucoma (19). Here, a morphometric study of the calcarine area was made in nine patients with retinal pathologies, including four with hereditary pigmentary degeneration of the retina. Wider calcarine fissures were reported in the patients group, particularly in the anterior and middle portions that are consistent with the peripheral VFD. However, visual field measurements were not performed to characterise the visual level of impairment of these patients and different pathologies were included in the study.

The present work aims to determine whether progressive peripheral vision loss in RP patients with partially preserved visual input leads to structural changes not only in the visual cortex, but also in the whole brain. This question is relevant as this may be the first whole brain morphometry study on peripheral VFD caused by a single retinal degeneration disorder. Whereas in glaucoma there is a progressive retinal ganglion cell loss and optic nerve damage, in RP there is a primary photoreceptor degeneration of the retina. For that purpose, a whole brain VBM analysis was applied to investigate GM abnormalities in patients with peripheral VFD due to RP.

Materials and methods

Subjects

Twenty-eight Retinitis Pigmentosa patients with peripheral vision loss were recruited from the Ophthalmology Department at Coimbra Hospital and University Centre (CHUC). Forty-five age- and gender-matched controls were recruited among the volunteers' database of the Institute for Biomedical Imaging and Life Sciences (IBILI) of the Faculty of Medicine, University of Coimbra, Portugal. All participants underwent an ophthalmologic examination (visual acuity assessment, automated perimetry and optical coherence tomography) and a structural magnetic resonance scanning. Patients with other neuro-ophthalmological or organic brain disorder were excluded from the study. One patient could not perform the MRI examination, being consequently excluded. Twenty-seven RP patients (12 female, 15 male; mean age 42.4 years; range 20-66 years) were finally included (Table 1 and 2). Controls were age- and gender-matched with RP patients and had no history of neurological disorders. Exclusion criteria included alterations in the ophthalmologic examination (automated perimetry and optical coherence tomography), ophthalmological disorders known a priori and alterations in the magnetic resonance scanning. Controls were required to have normal vision (visual acuity in both eyes 1.1 ± 0.2 decimals). Four subjects were excluded due to alterations on the ophthalmological examination and one subject was excluded due to lack of quality of the MRI acquisition. Forty healthy controls (19 female, 21 male; mean age 40 years; range 22-69 years) were included (Table 2).

The study was conducted in accordance to the Declaration of Helsinki and was approved by the Ethics Commission of Faculty of Medicine of University of Coimbra. Written informed consent was obtained from all participants.

Table 1 - Retinitis Pigmentosa characteristics.

Subject	Age (years)	Gender	Handedness	Age of disease onset (years)	Duration of disease (years)	Visual acuity (decimals)		Retinal thickness (µm)		RNFL thickness (µm)		Visual field diameter (angles)		Mean deficit (dB)	
						RE	LE	RE	LE	RE	LE	RE	LE	RE	LE
1	42	M	R	18	24	0.50	0.60	200	194	5	100	5	10	23.2	22.4
2	34	F	R	3	31	0.60	0.30	265	281	20	101	20	20	20.1	20.3
3	58	M	n/a	14	44	<0.05	<0.05	206	209	n/a[b]	53	n/a[b]	n/a[b]	n/a[a]	n/a[a]
4	38	F	R	6	32	0.28	0.80	221	216	25	133	25	25	16.9	18.1
5	45	F	R	39	6	0,66	0.80	184	192	10	76	10	10	14.9	15.4
6	47	F	R	14	33	0.40	0.33	250	239	5	88	5	n/a[a]	22.3	n/a[a]
7	35	M	R	6	29	0.50	0.90	243	226	10	89	10	10	22.0	21.9
8	41	M	RL	11	30	0.66	0.50	209	218	10	69	10	10	23.0	22.7
9	29	M	R	6	23	0.40	0.40	185	189	10	92	10	10	22.8	23.1
10	50	M	L	8	42	0.40	0.66	207	205	25	79	25	25	17.4	17.7
11	63	M	R	45	18	0.40	0.12	219	223	10	82	10	10	18.6	18.9
12	50	M	RL	16	34	0.50	0.50	203	201	10	70	10	10	20.0	20.2
13	61	M	n/a	10	51	0.60	0.30	274	268	10	70	10[c]	10[c]	-30.1[c]	-29.9[c]
14	20	M	RL	6	14	0.66	0.66	228	225	15	106	15	20	21.2	20.5
15	50	F	R	29	21	0.50	0.40	222	224	10	95	10	10	12.7	16.3
16	63	F	R	10	53	0.12	0.20	236	242	n/a[b]	86	n/a[b]	n/a[b]	n/a[a]	n/a[a]
17	66	F	R	18	48	0.28	0.12	291	295	48	91	48	48	4.4	5.2
18	52	M	R	7	45	<0.05	<0.05	227	215	n/a[b]	95	n/a[b]	n/a[b]	n/a[a]	n/a[a]
19	28	F	R	15	13	0.60	0.50	198	197	40	95	40	40	14.5	13.9
20	23	M	R	16	7	0.66	0.50	266	254	10	130	10	10	21.8	22.1
21	25	M	R	14	11	0.50	0.40	245	242	40	101	40	40	11.0	11.5
22	66	F	R	27	39	0.50	0.50	248	254	10	95	10	10	19.5	19.6
23	23	F	R	1	22	0.33	0.20	n/a[a]	n/a[a]	20	n/a[a]	20	20	21.4	21.3
24	36	M	R	26	10	0.20	0.33	308	291	n/a[b]	127	n/a[b]	n/a[b]	n/a[a]	n/a[a]
25	38	F	R	32	6	0.40	1.00	258	249	20	128	20	20	16.8	17.4
26	32	M	R	12	20	0.40	0.40	229	240	10	102	10	10	22.8	22.6
27	31	M	R	1	30	0.40	0.80	268	273	48	92	48	48	1.7	1.0

Characteristics of the patient group were age, gender, handedness, age of disease onset, duration of disease, visual acuity (expressed in decimals), retinal thickness (expressed in µm), RNFL thickness (expressed in µm), visual field (expressed in angles) and mean deficit of the visual field (expressed in decibel). M = male; F = female; R = Right; RE = right eye; RL = Right and left; L = Left; LE = left eye; RNFL = retinal nerve fiber layer; n/a = not available. [a]Patient with missing data. [b] Patient could not perform the exam. [c]Patient evaluated with Humphrey Field Analyzer.

Table 2 - Baseline subjects characteristics.

Characteristic	RP	Control	p Value
Age, years	42.4 ± 14.2	40.0 ± 13.0	0.473
Gender (male/female)	16/11	21/19	0.585
Handedness (right/left/both)[a]	21/1/3	33/2/4	0.370
Visual acuity of the left eye, decimal [b]	0.5 ± 0.2	1.1 ± 0.2	0.000
Visual acuity of the right eye, decimal [b]	0.5 ± 0.1	1.1 ± 0.2	0.000
RNFL thickness of the left eye, µm [c]	94.0 ± 19.7	94.4 ± 9.7	0.925
RNFL thickness of the right eye, µm [c]	95.4 ± 25.1	95.0 ± 10.7	0.940
Retinal thickness of the left eye, µm [c]	233.1 ± 30.8	287.4 ± 12.4	0.000
Retinal thickness of the right eye, µm [c]	234.2 ± 32.1	284.7 ± 22.0	0.000

Characteristics of the patient and control groups were age, gender, handedness, visual acuity, RNFL thickness and retinal thickness of both eyes (values are Mean+-Standard Deviation). RNFL = retinal nerve fiber layer. [a]2 patients with missing data. [b]2 controls with missing data. [c]5 controls and 1 patient with missing data. Significance level at $p < 0.05$.

Ophthalmic examination

All participants underwent an ophthalmic examination including visual acuity assessment, visual fields assessment with automated perimeter and retinal thickness and retinal nerve fiber layer (RNFL) thickness measurements with optical coherence tomography (OCT) (Table 1 and 2). All assessments were performed in each eye separately.

For each participant, visual acuity was determined using a 5-meter projected decimal chart. The right eye and left eye were evaluated separately with the same chart, apart for lines 1.0 decimal and 1.33 decimals, which could be presented with different optotypes for each eye. When visual acuity was so low that the patient was unable to read any of the largest letters or even count fingers, vision was tested with hand motion visual acuity and light perception testing.

Static visual fields were evaluated on all subjects except one using a MonCv3 multifunction perimeter (Metrovision) with a standardised program. A suprathreshold strategy (4 dB above the theoretical luminance threshold) was used for the 79 points tested in the central 24 degrees (radius) using a rapid thresholding strategy. When subjects could not execute the test due to narrow visual field, a central 12 degrees (radius) assessment was performed. Testing was always carried out with appropriate refractive correction. Fixation was monitored in real time by means of an integrated camera and controlled by the operator. Static visual field of one patient was evaluated with Humphrey Field Analyzer (Carl ZeissS Meditec) for the 10 central degrees due to unavailability of the MonCv3 multifunction perimeter on the day of examination. Despite being different, the characterisation of the visual fields size is similarly obtained from both equipment. Visual field extent was then estimated for each eye of each patient in angles of visual degree (diameter). The maximum diameter of visual field was approximately estimated, by defining the scotoma as the black region (0 dB of sensitivity) obtained in the static perimetry sensitivity map (Figure 1).

Frequency Domain Cirrus Ocular Coherence Tomography (OCT, Carl Zeiss Meditec AG, USA) with the software version 5.1.1.6 was performed to measure retinal thickness and RNFL thickness, in all participants. A macular scan with a resolution of 512×128 and an optic disc scan with a resolution of 200×200 were acquired (Figures 2 and 3).

Statistical analysis of demographic and visual data

The statistical analysis was performed by using IBM SPSS Statistics, version 23.0. Age and RNFL thickness of the right and left eyes were compared between patient and control groups by using a two-sample t-test. Gender and handedness comparisons between groups was performed using a Pearson's chi-square test. Visual acuity and retinal thickness of the right

and left eyes were compared between the study groups by performing a Mann-Whitney U test. All p values < 0.05 were considered statistically significant (Table 2).

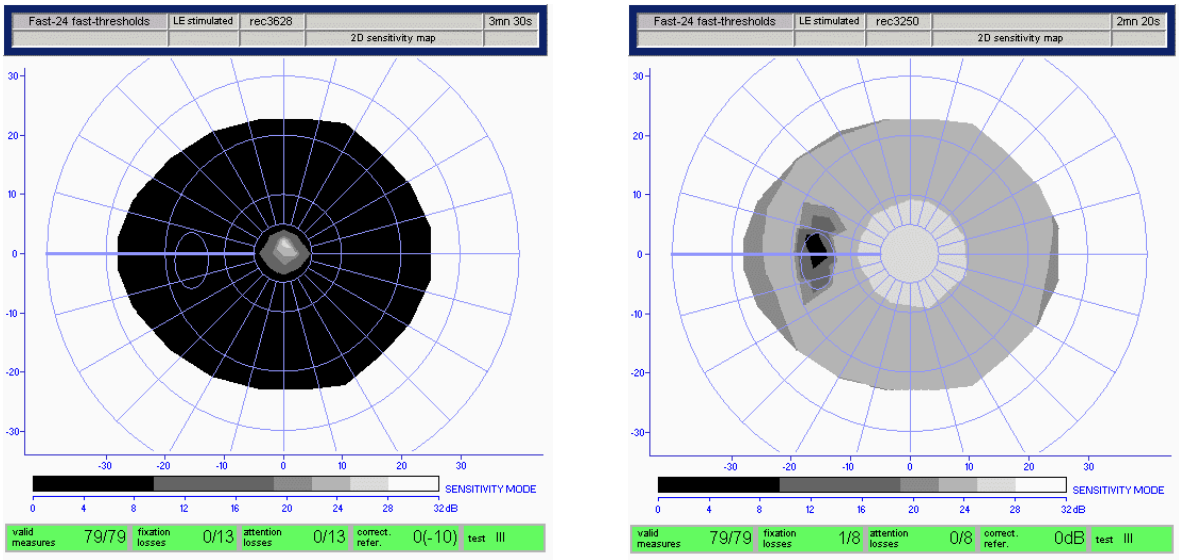

Figure 1 - Examples of static perimetry sensitivity maps using MonCv3 multifunction perimeter (Metrovision). **(A)** Visual field result of the left eye of a patient with Retinitis Pigmentosa (Subject 1 with visual field size of about 10º visual angle in diameter) . **(B)** Visual field result of the left eye of a control.

MRI acquisition

High-resolution brain anatomical images were acquired in a 3T Siemens TimTrio, using a 12-channel birdcage head coil. Two 6 minutes long T_1-weighted magnetization-prepared rapid acquisition with gradient echo (MPRAGE) sequences: repetition time (TR) 2.53s, echo time (TE) 3.42ms, flip angle (FA) 7°, field of view (FOV) 265 x 256 mm^2, resulting in 176 slices with 1 x 1x 1 mm^3. Additionally, brain scans of two patients and two controls were acquired in the same scanner but with different MPRAGE sequence parameters: repetition time (TR) 2.3s, echo time (TE) 2.98ms, flip angle (FA) 9°, field of view (FOV) 256 x 256 mm^2,

resulting in 160 slices with 1 x 1x 1 mm^3. Acquisition time was approximately 10 minutes for each sequence. Two anatomical sequences were acquired for each participant.

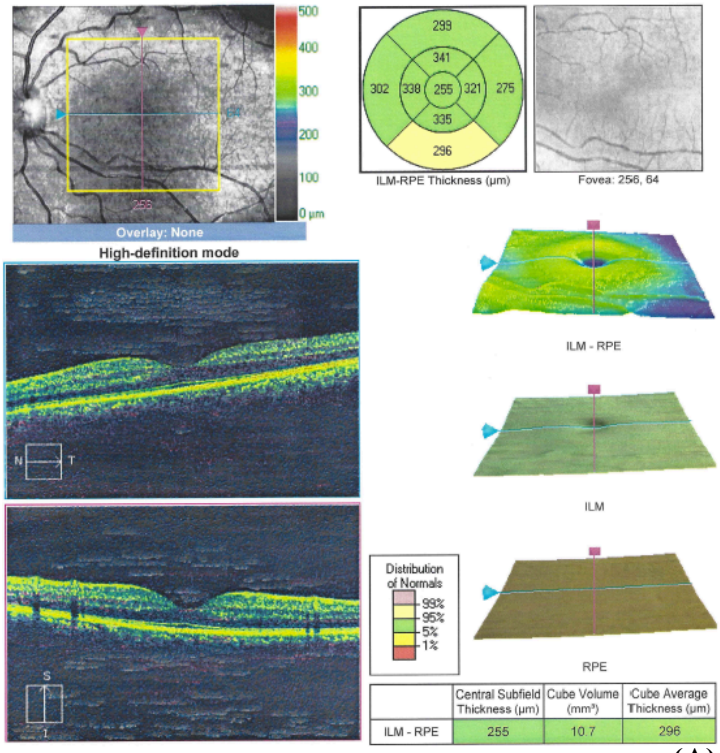

(A)

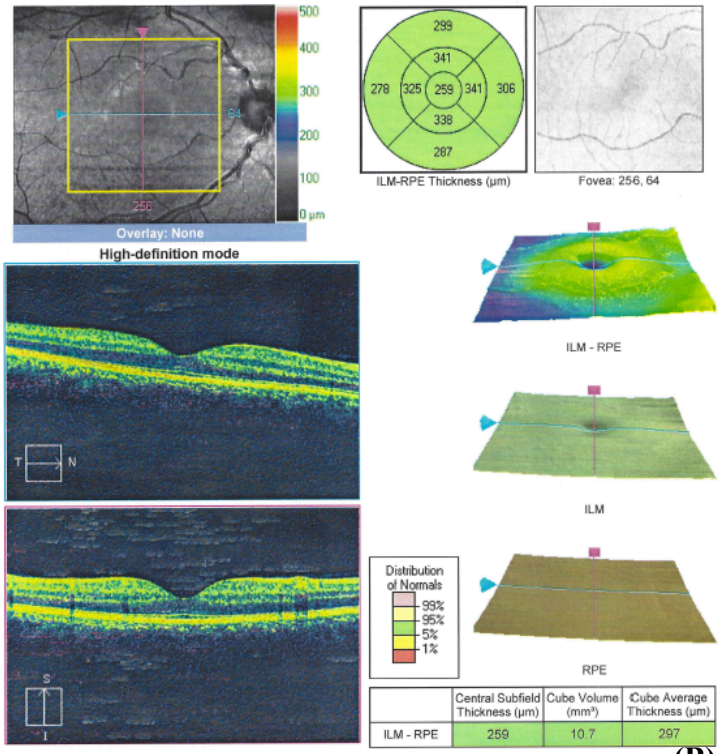

(B)

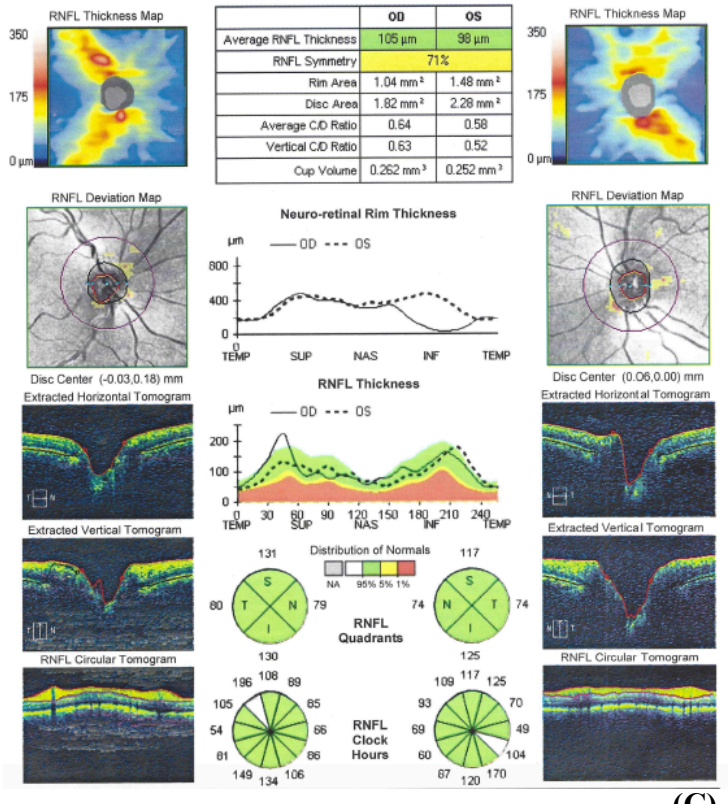

(C)

Figure 2 - Retinal and RNFL thickness measurements of a control subject with Frequency Domain Cirrus Ocular Coherence Tomography. **(A)** Macular thickness measurement of the left eye. **(B)** Macular thickness measurement of the right eye. **(C)** RNFL thickness measurement of both eyes. OD = Right eye; OE = Left eye.

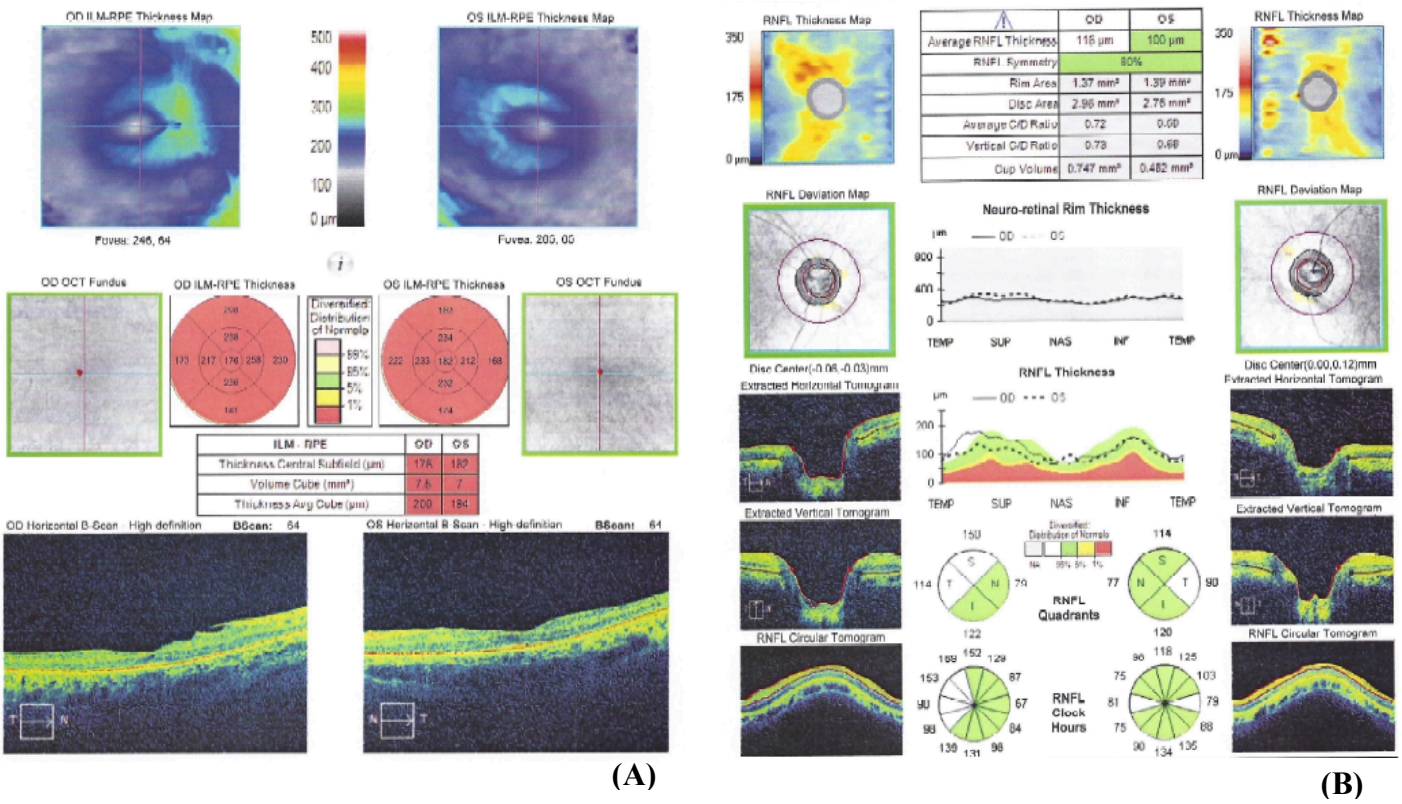

Figure 3 - Retinal and RNFL thickness measurements of a Retinitis Pigmentosa patient (Subject 1) with Frequency Domain Cirrus Ocular Coherence Tomography. **(A)** Macular thickness measurement of both eyes. **(B)** RNFL thickness measurement of both eyes. OD = Right eye; OE = Left eye.

VBM data analysis

The T1 weighted images were processed using a standalone SPM8 (Statistical Parametric Mapping) version (http://www.fil.ion.ucl.ac.uk/), compiled with a MATLAB compiler (The Math-Works, Inc., Natick, MA), in order to perform VBM analyses.

Firstly, every scan was aligned to the anterior commissure. Then, the unified segmentation algorithm (20) was used to normalise, segment and modulate the images as follow: all T1-weighted images were registered to the Montreal Neurological Institute (MNI) coordinate system by registering the MR images to the ICBM 152 template. Normalised images were segmented into grey matter (GM), white matter (WM) and cerebrospinal fluid (CSF). The

GM images were modulated to correct for GM volume change due to nonlinear registration. Additionally, the normalised, segmented, modulated GM images were smoothed with a Gaussian kernel with 8 mm of full width at half maximum (FWMH) to ensure the normality of the data. Finally, voxelwise statistical analyses were applied in these preprocessed GM images.

In the statistical analyses, GM volume alterations were assessed by comparing RP patients and controls (CTL) using two different contrasts (CTL > RP and RP > CTL) and the standard general linear module (GLM) implementation in SPM8 for independent two-sample t-tests. Statistical parametric maps were created by applying a significant threshold of $p < 0.001$, uncorrected for multiple comparisons on voxel level, and a cluster correction of $k = 100$. Results were also thresholded at p (family-wise error - FWE) < 0.05, corrected for multiple comparisons, and a cluster correction of $k = 20$ was applied. Even though, participants were age- and gender-matched, age, gender and total intra-cranial volume (TIV) were added as covariates to the analysis to exclude any possible confounding effects.

Results

Demographic and visual data

RP patients and controls were age, gender and handedness-matched ($p > 0.05$, Table 2). Significant statistical differences were identified for visual acuity and retinal thickness of both eyes, between groups ($p < 0.05$, Table 2). No significant statistical difference was observed for RNFL thickness of both eyes, between RP patients and controls ($p > 0.05$, Table 2).

VBM data

Figure 4 shows the statistical parametric maps of grey matter atrophy in RP patients when the significant threshold of $p < 0.001$, uncorrected for multiple comparisons, and the cluster correction of $k = 100$ were applied. The GM atrophy is more pronounced in the left hemisphere and involved the following brain brains: left pericalcarine, cuneus, posterior cingulate, pericalcarine right and lingual (Table 3).

Figure 5 shows the results obtained when the p (family-wise error - FWE) < 0.05 threshold, corrected for multiple comparisons, and the cluster correction of $k = 20$ were applied. This analysis provides confirmatory support of the findings observed before in the left pericalcarine cortex, cuneus and lingual gyrus (Table 4).

The analysis with the contrast RP > CTL yielded no significant results at the same thresholds and is therefore not presented.

Table 3 - Location and peak significance of GM atrophy in RP patients when compared with controls ($p < 0.001$, uncorrected for multiple comparisons, and $k = 100$).

Voxels	Peak *t* value	*p* value (uncorrected, except for cluster level of 100)	Talairach coordinates (x, y, z) (mm)	Brain areas
315	3.2909	< 0.001	-10, -84, 4	Occipital lobe, Left hemisphere, Pericalcarine left, Cuneus, Right hemisphere, Posterior cingulate, Pericalcarine right, Lingual.

Table 4 - Location and peak significance of GM atrophy in RP patients when compared with controls ($p < 0.05$, FWE corrected for multiple comparisons, and $k = 20$).

Voxels	Peak *t* value	*p* value (FWE correction)	Talairach coordinates (x, y, z) (mm)	Brain areas
66	6.1435	< 0.05	-8, -86, 2	Left hemisphere, Occipital lobe, Pericalcarine left, Cuneus, Lingual.

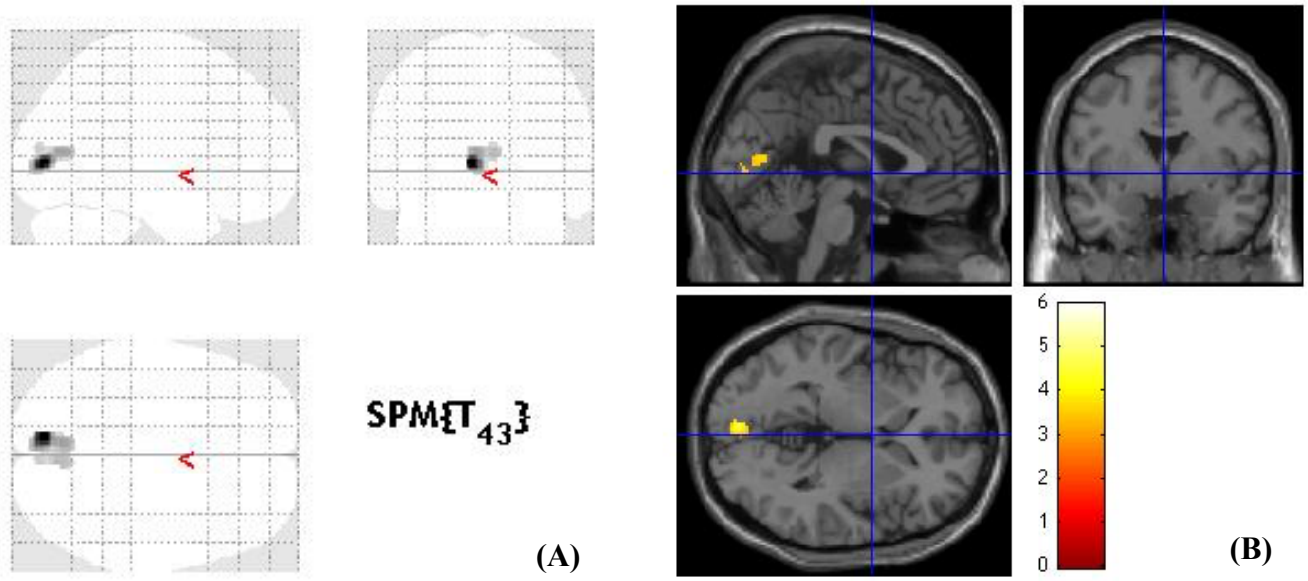

Figure 4 - Brain areas with significant GM atrophy in RP patients when compared with controls ($p < 0.001$, uncorrected for multiple comparisons, and $k = 100$). **(A)** In the *t*-statistic cluster map, the black / grey areas represent GM atrophy. **(B)** The coloured bar encodes areas of significant GM volume differences between RP and controls subjects, white / yellow represents more significant differences (higher *t*-values) and red indicates less significant differences (lower *t*-values). Colour represents areas with GM atrophy in RP patients.

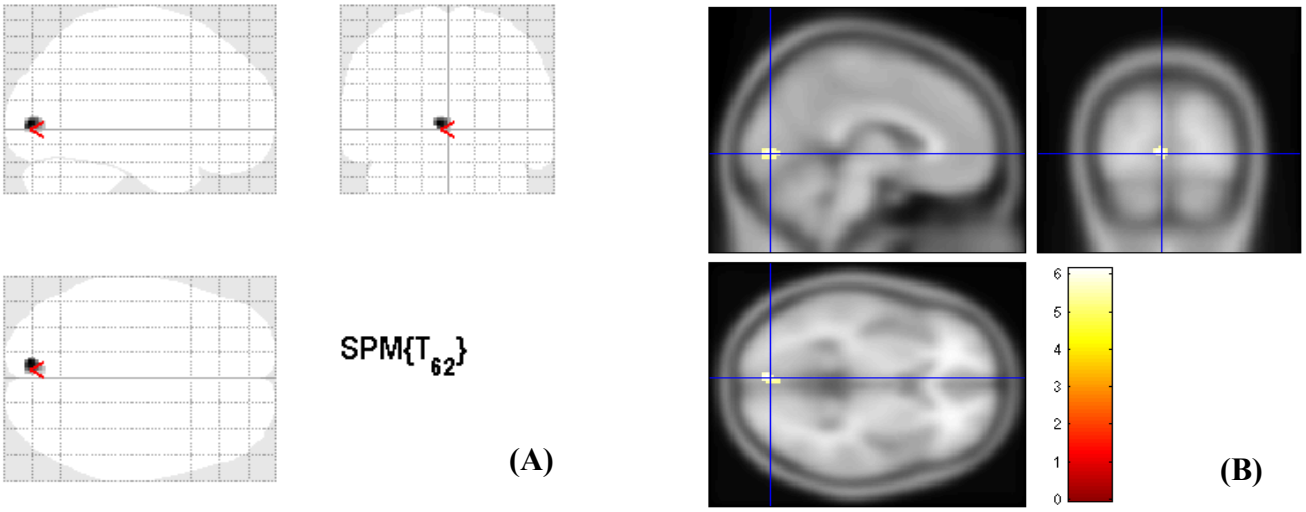

Figure 5 - Brain areas with significant GM atrophy in RP patients when compared with controls ($p < 0.05$, FWE corrected for multiple comparisons, and $K = 20$). **(A)** In the *t*-statistic cluster map, the black / grey areas represent GM atrophy. **(B)** The coloured bar encodes areas of significant GM volume differences between RP and controls subjects, white / yellow represents more significant differences (higher *t*-values) and red indicates less significant differences (lower *t*-values). Colour represents areas with GM atrophy in RP patients.

Discussion

The results show that Retinitis Pigmentosa patients with partially preserved vision have significant grey matter (GM) atrophy in several structural components of the visual primary and association cortices, when compared to healthy controls. To our knowledge, this is the first whole brain morphometry study in this pathology.

Regions with GM atrophy where the left pericalcarine cortex, cuneus gyrus, posterior cingulate gyrus, right pericalcarine cortex and lingual gyrus ($p < 0.001$, uncorrected for multiple comparisons, except for the cluster correction approach). The differences were more pronounced in the left hemisphere. As whole brain structural MRI data involves a large number of statistic comparisons, a FWE correction for multiple comparisons was applied ($p <$

0.05), limiting the presence of false positives in the results (type I error). Nevertheless, GM atrophy was observed in the left pericalcarine cortex, cuneus gyrus and lingual gyrus. This more conservative analysis corroborates the observed results of GM atrophy in the primary visual cortex.

The visual cortex is organised into retinotopic maps. In the retina, each visual field representation has receptive fields at nearby locations in the image. Thus, these topologic maps preserve the spatial arrangement of the retinal image in the primary visual cortex (V1), where adjacent stimuli in the visual field are represented in adjacent positions in the visual cortex. If progressive VFD occur, the corresponding part of the visual cortex gradually loses this input. Thus, continued visual input loss due to VFD can result in structural changes at the visual cortex level, particularly in V1 (21-23). Indeed, the peripheral visual field defect characteristic of RP corresponds to a partial loss of input to the visual cortex. This loss of stimulation is one possible explanation for the GM atrophy observed in the visual cortex, as proposed in studies on other hereditary retinal dystrophies and AMD (11, 13). The brain areas where GM atrophy was observed correspond to areas responsible for processing visual information. The primary visual cortex (V1), which receives direct input from the retinogeniculate pathway and is responsible for early visual processing, comprises the pericalcarine cortex and extends into the cuneus and lingual gyrus. These areas have shown GM atrophy in RP patients with partially preserved vision, which indicates widespread atrophy of V1 in this pathology. The posterior cingulate gyrus is included in the limbic lobe, a component of the Papez circuit and functionally important in emotions and memory, such as spatial short-term memory. The cingulate gyrus, which also presented GM atrophy in RP patients when compared to controls (albeit only at the cluster correction level), has extensive connections with visual-association areas of the parietal, occipital and temporal lobes. These connections can be decreased due to loss of visual input, leading to atrophy of the cingulate

gyrus. Thus, possible explanations for the observed GM atrophy in the visual cortex are disuse-driven neuronal atrophy and/or transneuronal degeneration (24). The alterations of the structure of afferent visual pathways in RP retinal degeneration have been investigated by measuring retinal nerve fiber layer (RNFL) and retinal thickness, using optical coherence tomography (OCT). While retinal thinning is consensual across studies (25-27), the RNFL findings have been somewhat contradictory: RNFL thickness was reported to be increased, decreased or maintained within normal limits, in several studies (27-29). However, in the present study, mean RNFL thickness of RP patients was similar to the control group, in both eyes (Table 2), which is in favour of axonal integrity of the optic nerve at least when vision is still partially preserved, as was the case for this study. Optic pathway trans-synaptic neurodegeneration (Wallerian degeneration) has been well established in patients with glaucoma-induced retinal ganglion cells (RGC) damage. In macular degeneration, volumetric loss of the visual pathway has also been observed (17, 30, 31). Indeed, the adverse effect of photoreceptor degeneration (first-order neuron) affecting RGC (third-order neurons) was proposed as a possible explanation (14). Further studies will be needed to determine whether white matter volume and fibre connectivity are altered by partial visual deprivation resulting from the retinal degeneration characteristic of RP.

Contrarily to some studies in glaucoma (15, 16, 18), GM hypertrophy was not observed in RP patients when compared to controls, which does not support the hypothesis of cerebral plasticity and cortical remodelling in this pathology.

Individual variability in grey matter volume due to differences in overall head size was taken into account by adding total intra-cranial volume as covariate to the statistical analysis. Although the group mean ages were not significantly different (Table 2), age was modelled as covariate. Indeed, this study involved older patients, so there is a possibility that an ageing effect may be present, influencing the reported results (32, 33). Gender was also added as a

covariate to the analysis to exclude any possible confounding effects. Having included age, gender and head size as covariables, reducing the individual variability in GM volumetric measurement (33), the most parsimonious explanation for the GM atrophy observed in patients is directly related with the primary photoreceptor degeneration, known to be a characteristic of Retinitis Pigmentosa. Potential limitations of the voxel-based analysis should be mentioned (5-7). Firstly, by registering all T1-weighted images in the same coordinate system, misregistration due to brain anatomical variability can occur. Secondly, motion artefact during the MRI acquisition can result in registration and segmentation errors. Thirdly, fine-scale anatomical localisation can be compromised due to spatial normalisation and smoothing.

These results support the hypothesis that atrophy and degeneration of the visual cortex can occur in patients with partially preserved vision and not only when blindness is settled. These findings may have important clinical implications in disease management, as a neurodegenerative pathophysiology may also be present early in the course of the disease. As such, slowing the progression of retinal degeneration with neuroprotective treatments (nutritional and drug supplements) might be a potentially promising therapeutic strategy, by preventing a further decline in visual function. Current investigational treatment modalities, such as gene replacement therapy, retinal or stem cell transplantation, pharmacologic neurotrophic factors and neuroprosthetic devices should be implemented early in the course of the disease to avoid progression to visual cortical atrophy (1, 2, 34).

Conclusion

Partial retinal input deprivation in Retinitis Pigmentosa patients leads to structural changes in the human cortex, namely grey matter atrophy in primary and association visual areas. Thus, cortical structural alterations due to vision loss occur early during Retinitis Pigmentosa progress and not only when blindness is settled. Retinitis Pigmentosa has been clinically managed as an ophthalmological disease. However, the gray matter atrophy observed in the visual cortex may alert clinicians to the possible neurodegenerative mechanisms involved in the pathology. Further studies will be needed to understand the mechanisms of gray matter atrophy in the visual cortex, especially on the integrity of the visual pathways in Retinitis Pigmentosa.

Agradecimentos

Agradeço ao meu orientador Professor Doutor Miguel Castelo-Branco pela oportunidade de trabalhar na área fascinante das Neurociências, pelo sentido crítico e pelos ensinamentos.

Agradeço ao Professor Doutor Eduardo Silva pela seleção dos doentes da sua consulta para o projeto.

Agradeço ao meu co-orientador Fábio Ferreira e à Andreia Pereira pela disponibilidade, pelo incentivo e pela palavra amiga.

Agradeço à Sónia Ferreira e ao Bruno Quendera pela aquisição dos dados imagiológicos e visuais dos participantes.

Um especial agradecimento aos participantes pela disponibilidade e interesse no projecto.

Por último, um obrigada aos meus pais, os meus ídolos da Medicina e da vida, pelo apoio incondicional e por tanto acreditarem em mim. Um obrigada também à Beatriz, ao João e à Eduarda pelo encorajamento e pela companhia sempre presente.

Este trabalho foi financiado pela Fundação para a Ciência e Tecnologia através dos projetos E-Rare2-SAU/0001/2008, E-Rare4/0001/2012 e UID/NEU/04539/2013

References

1. Hartong DT, Berson EL, Dryja TP. Retinitis pigmentosa. Lancet. 2006;368(9549):1795-809.
2. Hamel C. Retinitis pigmentosa. Orphanet journal of rare diseases. 2006;1:40.
3. Cottet S, Schorderet DF. Mechanisms of apoptosis in retinitis pigmentosa. Current molecular medicine. 2009;9(3):375-83.
4. Herse P. Retinitis pigmentosa: visual function and multidisciplinary management. Clinical & experimental optometry : journal of the Australian Optometrical Association. 2005;88(5):335-50.
5. Andrea Mechelli CJP, Karl J. Friston, John Ashburner. Voxel-Based Morphometry of the Human Brain: Methods and
Applications. Current Medical Imaging Reviews. 2005;1:00-.
6. Ashburner J, Friston KJ. Voxel-based morphometry--the methods. NeuroImage. 2000;11(6 Pt 1):805-21.
7. Whitwell JL. Voxel-based morphometry: an automated technique for assessing structural changes in the brain. The Journal of neuroscience : the official journal of the Society for Neuroscience. 2009;29(31):9661-4.
8. Park HJ, Lee JD, Kim EY, Park B, Oh MK, Lee S, et al. Morphological alterations in the congenital blind based on the analysis of cortical thickness and surface area. NeuroImage. 2009;47(1):98-106.
9. Jiang J, Zhu W, Shi F, Liu Y, Li J, Qin W, et al. Thick visual cortex in the early blind. The Journal of neuroscience : the official journal of the Society for Neuroscience. 2009;29(7):2205-11.
10. Voss P, Pike BG, Zatorre RJ. Evidence for both compensatory plastic and disuse atrophy-related neuroanatomical changes in the blind. Brain : a journal of neurology. 2014;137(Pt 4):1224-40.
11. Boucard CC, Hernowo AT, Maguire RP, Jansonius NM, Roerdink JB, Hooymans JM, et al. Changes in cortical grey matter density associated with long-standing retinal visual field defects. Brain : a journal of neurology. 2009;132(Pt 7):1898-906.
12. Barcella V, Rocca MA, Bianchi-Marzoli S, Milesi J, Melzi L, Falini A, et al. Evidence for retrochiasmatic tissue loss in Leber's hereditary optic neuropathy. Human brain mapping. 2010;31(12):1900-6.
13. Plank T, Frolo J, Brandl-Ruhle S, Renner AB, Hufendiek K, Helbig H, et al. Gray matter alterations in visual cortex of patients with loss of central vision due to hereditary retinal dystrophies. NeuroImage. 2011;56(3):1556-65.
14. Hernowo AT, Prins D, Baseler HA, Plank T, Gouws AD, Hooymans JM, et al. Morphometric analyses of the visual pathways in macular degeneration. Cortex; a journal devoted to the study of the nervous system and behavior. 2014;56:99-110.
15. Li C, Cai P, Shi L, Lin Y, Zhang J, Liu S, et al. Voxel-based morphometry of the visual-related cortex in primary open angle glaucoma. Current eye research. 2012;37(9):794-802.
16. Chen WW, Wang N, Cai S, Fang Z, Yu M, Wu Q, et al. Structural brain abnormalities in patients with primary open-angle glaucoma: a study with 3T MR imaging. Investigative ophthalmology & visual science. 2013;54(1):545-54.
17. Zikou AK, Kitsos G, Tzarouchi LC, Astrakas L, Alexiou GA, Argyropoulou MI. Voxel-based morphometry and diffusion tensor imaging of the optic pathway in primary open-angle glaucoma: a preliminary study. AJNR American journal of neuroradiology. 2012;33(1):128-34.

18. Williams AL, Lackey J, Wizov SS, Chia TM, Gatla S, Moster ML, et al. Evidence for widespread structural brain changes in glaucoma: a preliminary voxel-based MRI study. Investigative ophthalmology & visual science. 2013;54(8):5880-7.
19. Kitajima M, Korogi Y, Hirai T, Hamatake S, Ikushima I, Sugahara T, et al. MR changes in the calcarine area resulting from retinal degeneration. AJNR American journal of neuroradiology. 1997;18(7):1291-5.
20. Ashburner J, Friston KJ. Unified segmentation. NeuroImage. 2005;26(3):839-51.
21. Wandell BA, Brewer AA, Dougherty RF. Visual field map clusters in human cortex. Philosophical transactions of the Royal Society of London Series B, Biological sciences. 2005;360(1456):693-707.
22. Wandell BA, Dumoulin SO, Brewer AA. Visual field maps in human cortex. Neuron. 2007;56(2):366-83.
23. Wandell BA, Winawer J. Imaging retinotopic maps in the human brain. Vision research. 2011;51(7):718-37.
24. Prins D, Hanekamp S, Cornelissen FW. Structural brain MRI studies in eye diseases: are they clinically relevant? A review of current findings. Acta ophthalmologica. 2015.
25. Triolo G, Pierro L, Parodi MB, De Benedetto U, Gagliardi M, Manitto MP, et al. Spectral domain optical coherence tomography findings in patients with retinitis pigmentosa. Ophthalmic research. 2013;50(3):160-4.
26. Battaglia Parodi M, La Spina C, Triolo G, Riccieri F, Pierro L, Gagliardi M, et al. Correlation of SD-OCT findings and visual function in patients with retinitis pigmentosa. Graefe's Archive for Clinical and Experimental Ophthalmology. 2015:1-5.
27. Hood DC, Lin CE, Lazow MA, Locke KG, Zhang X, Birch DG. Thickness of receptor and post-receptor retinal layers in patients with retinitis pigmentosa measured with frequency-domain optical coherence tomography. Investigative ophthalmology & visual science. 2009;50(5):2328-36.
28. Oishi A, Ogino K, Nakagawa S, Makiyama Y, Kurimoto M, Otani A, et al. Longitudinal analysis of the peripapillary retinal nerve fiber layer thinning in patients with retinitis pigmentosa. Eye (London, England). 2013;27(5):597-604.
29. Anastasakis A, Genead MA, McAnany JJ, Fishman GA. Evaluation of retinal nerve fiber layer thickness in patients with retinitis pigmentosa using spectral-domain optical coherence tomography. Retina (Philadelphia, Pa). 2012;32(2):358-63.
30. Garaci FG, Bolacchi F, Cerulli A, Melis M, Spanò A, Cedrone C, et al. Optic Nerve and Optic Radiation Neurodegeneration in Patients with Glaucoma: In Vivo Analysis with 3-T Diffusion-Tensor MR Imaging. Radiology. 2009;252(2):496-501.
31. Hernowo AT, Boucard CC, Jansonius NM, Hooymans JMM, Cornelissen FW. Automated Morphometry of the Visual Pathway in Primary Open-Angle Glaucoma. Investigative ophthalmology & visual science. 2011;52(5):2758-66.
32. Salat DH, Buckner RL, Snyder AZ, Greve DN, Desikan RS, Busa E, et al. Thinning of the cerebral cortex in aging. Cerebral cortex (New York, NY : 1991). 2004;14(7):721-30.
33. Barnes J, Ridgway GR, Bartlett J, Henley SM, Lehmann M, Hobbs N, et al. Head size, age and gender adjustment in MRI studies: a necessary nuisance? NeuroImage. 2010;53(4):1244-55.
34. Shintani K, Shechtman DL, Gurwood AS. Review and update: current treatment trends for patients with retinitis pigmentosa. Optometry (St Louis, Mo). 2009;80(7):384-401.